The Basis for Strain-Dependent Rat Aldehyde Dehydrogenase 1A7 (*ALDH1A7*) Gene Expression [S]

Katerina Touloupi, [iD]Jenni Küblbeck, [iD]Angeliki Magklara, [iD]Ferdinand Molnár, [iD]Mika Reinisalo, [iD]Maria Konstandi, [iD]Paavo Honkakoski,[1] and [iD]Periklis Pappas[2]

Departments of Pharmacology (K.T., M.K., P.P.) and Clinical Chemistry (A.M.), Faculty of Medicine, School of Health Sciences, University of Ioannina, and Department of Biomedical Research, Institute of Molecular Biology and Biotechnology, Foundation of Research and Technology (A.M.), Ioannina, Greece; School of Pharmacy, Faculty of Health Sciences, University of Eastern Finland, Kuopio, Finland (J.K., F.M., M.R., P.H.);Department of Biology, School of Science and Technology, Nazarbayev University, Nur-Sultan City, Kazakhstan (F.M.); Division of Pharmacotherapy and Experimental Therapeutics, UNC Eshelman School of Pharmacy, University of North Carolina at Chapel Hill, Chapel Hill, North Carolina (P.H.)

Received May 30, 2019; accepted September 6, 2019

ABSTRACT

Aldehyde hydrogenases (ALDHs) belong to a large gene family involved in oxidation of both endogenous and exogenous compounds in mammalian tissues. Among ALDHs, the rat *ALDH1A7* gene displays a curious strain dependence in phenobarbital (PB)-induced hepatic expression: the responsive **RR** strains exhibit induction of both ALDH1A7 and CYP2B mRNAs and activities, whereas the nonresponsive **rr** strains show induction of CYP2B only. Here, we investigated the responsiveness of *ALDH1A1*, *ALDH1A7*, *CYP2B1*, and *CYP3A23* genes to prototypical P450 inducers, expression of nuclear receptors CAR and pregnane X receptor, and structure of the *ALDH1A7* promoter in both rat strains. ALDH1A7 mRNA, associated protein and activity were strongly induced by PB and modestly induced by pregnenolone 16α-carbonitrile in the **RR** strain but negligibly in the **rr** strain, whereas induction of ALDH1A1

and P450 mRNAs was similar between the strains. Reporter gene and chromatin immunoprecipitation assays indicated that the loss of *ALDH1A7* inducibility in the **rr** strain is profoundly linked with a 16-base pair deletion in the proximal promoter and inability of the upstream DNA sequences to recruit constitutive androstane receptor-retinoid X receptor heterodimers.

SIGNIFICANCE STATEMENT

Genetic variation in rat *ALDH1A7* promoter sequences underlie the large strain-dependent differences in expression and inducibility by phenobarbital of the aldehyde dehydrogenase activity. This finding has implications for the design and interpretation of pharmacological and toxicological studies on the effects and disposition of aldehydes.

Introduction

The aldehyde dehydrogenases (ALDHs) are present in all taxonomic groups, and they are involved in the irreversible oxidation of endogenous and exogenous aldehydes (Sophos et al., 2001). Their functionality extends far beyond enzymatic detoxification processes because they participate in the growth, differentiation, and survival of cells and in the synthesis of biomolecules, such as retinoic acid, betaine, and

γ-aminobutyric acid. ALDHs may also serve as biomarkers for certain cancer types and Parkinson disease (Westerlund et al., 2005; Jackson et al., 2011). Among the 21 genes of the rat *ALDH* gene superfamily (Jackson et al., 2011), the cytosolic isoforms ALDH1A1, 2, 3, and 7 are involved in the metabolism of, for example, aliphatic aldehydes and retinal and cyclophosphamide (Kathmann et al., 2000; Alnouti and Klaassen, 2008). Among these isoforms, rat ALDH1A1 and ALDH1A7 are highly homologous and display similar tissue-expression patterns, with high mRNA levels reported in the liver, lung, and kidneys (Marselos et al., 1987; Hsu et al., 1999; Kathmann et al., 2000). Moreover, hepatic expression of rat ALDH1A1 and 1A7 isozymes is induced by phenobarbital (PB), a prototypical inducer of several cytochrome P450 (P450) enzymes.

In rodents, PB is known to induce many P4540s and other drug-metabolizing enzymes and transporters via the nuclear receptor (NR) constitutive androstane receptor (CAR), whereas many drugs induce their expression by activation of

ABBREVIATIONS: ALDH, aldehyde dehydrogenase; bp, base pair; CAR, constitutive androstane receptor; ChIP, chromatin immunoprecipitation; kbp, kilobase pair; NR, nuclear receptor; P450, cytochrome P450; PB, phenobarbital; PCN, pregnenolone 16α-carbonitrile; PXR, pregnane X receptor; RT-PCR, reverse transcription-polymerase chain reaction; RU486, mifepristone; RXR, retinoid X receptor; SDS, sodium dodecyl sulfate; TCPOBOP, 1,4-bis[(3,5-dichloropyridyloxy)]benzene; TF, transcription factor; TSS, transcription start site.

the pregnane X receptor (PXR) (Honkakoski and Negishi, 2000; Chai et al., 2013). Others reported that selective CAR or PXR activators modestly increased (2- to 3.5-fold) *Aldh1a1* and *Aldh1a7* gene expression in the livers of wild-type mice but not in mice with disrupted *Car* or *Pxr* genes, whereas the expression of other *Aldh* family members was not appreciably affected by NR activation (Aleksunes and Klaassen, 2012). These findings indicate that the key NRs regulating drug-metabolizing enzymes are involved in the regulation of cytosolic ALDH1A isoforms.

The induction of cytosolic ALDH by PB has been investigated because of genetic strain differences in specific Long-Evans rat strains (Deitrich, 1971; Dunn et al., 1989; Kathmann et al., 2000). The extent of PB-elicited induction of rat liver cytosolic ALDH activity appears to be regulated by two alleles of a single autosomal locus. The dominant allele **R** confers responsiveness to PB, whereas the recessive allele **r** is nonresponsive. Homozygous responders (**RR**) exhibit maximal ALDH induction by PB, heterozygous rats (**Rr**) display a moderate induction and homozygous nonresponders (**rr**) show only a small, if any, increase of ALDH activity. Constitutive ALDH mRNA expression (initially termed *ALDH-PB*, now recognized as *ALDH1A7*) is detectable in both strains, but it is strongly inducible in only the **RR** rats. Interestingly, the expression of other PB-inducible enzymes, such as CYP2B1 and CYP2B2, reached similar levels in these strains after exposure to PB (Dunn et al., 1989; Pappas et al., 2001); however, the molecular basis for this ALDH-selective disparity in induction by PB remains unexplored to this day. To investigate this problem, we used the Wistar/Af/Han/Mol/Kuo/Io rat strain that is currently bred and maintained at University of Ioannina. This Wistar rat strain also exhibits discordant patterns of *ALDH1A* expression that are similar to the Long-Evans rat strains (Pappas et al., 1998; Pappas et al., 2001). The basal ALDH1A activity is ~2-fold greater, and its PB inducibility is markedly higher in the **RR** strain (>15-fold vs. 2.5-fold) compared with the **rr** strain. Here, we cloned and characterized *ALDH1A7* from both Wistar rat strains to identify the defect in PB induction and investigated its regulation by CAR and PXR.

Materials and Methods

Chemicals. Phenobarbital (PB) and mifepristone (RU486) were from Sigma-Aldrich (St. Louis, MO). Pregnenolone 16α-carbonitrile (PCN) was bought from SantaCruz Biotechnology (Heidelberg, Germany). Synthesis of the mouse CAR agonist 1,4-bis[(3,5-dichloropyridyloxy)]benzene (TCPOBOP) has been previously described (Honkakoski et al., 1996). All other chemicals were of the highest analytical grade.

Experimental Animal Model and Treatments. Wistar/Af/Han/Mol/Kuo/Io male rats (aged 3–5 months and weighing 170–230 g) were isolated and reproduced by inbreeding at the University of Ioannina, creating substrains that are responsive (**RR**) and nonresponsive (**rr**) to PB (Marselos, 1976). All animals were treated according to the European Communities Council Directive (86/609/EEC) and housed in groups of two or three in plastic cages under constant environmental conditions on a 12-hour light/dark cycle at ambient temperature and provided with chow and tap water ad libitum. All in vivo experiments were reviewed and approved by the Institutional Animal Care and Use Committee of the Medical School at the University of Ioannina (license number EL33BIO-exp01). For the multiple-dose study, 3-month old male rats (four per group) were injected intraperitoneally with selective activators of

CAR and PXR (Stanley et al., 2006): three doses of PB (80 mg/kg, dissolved in saline), four doses of PCN (50 mg/kg, dissolved in olive oil), or the corresponding vehicle. Animals were sacrificed by carbon asphyxiation 6 hours after the PB injection. For the time-response study, 3-month-old male rats were divided into groups of four and treated with a single dose of PB (80 mg/kg), PCN (50 mg/kg), or vehicle. Animals were sacrificed by carbon asphyxiation after 6, 12, or 24 hours of PB or PCN injection.

Total RNA Isolation, cDNA Synthesis, and Quantitative Reverse Transcription-Polymerase Chain Reaction. After decapitation, small liver samples were stored in RNAlater at −80°C until use. Total RNA was isolated with the Nucleospin RNA II total RNA isolation kit (Macherey-Nagel, Düren, Germany). RNA samples (1 μg) served as templates for cDNA synthesis using Quanti-Tect Reverse Transcription kit (Qiagen, Hilden, Germany). Analysis of liver mRNA levels was performed with real-time reverse transcription polymerase chain reaction (RT-PCR), based on the TaqMan protocol, by use of KAPA Probe Fast qPCR Master Mix (KAPA Biosystems, Wilmington, MA) and TaqMan Gene Expression Assay primers for rat ALDH1A1, ALDH1A7, CAR, PXR, CYP2B1, CYP3A23, and β-actin genes (Applied Biosystems, Foster City, CA). Amplification reactions (two replicate reactions per sample) were performed on the CFX96 real-time system and the C1000 thermal cycler (Bio-Rad Laboratories, Hercules, CA). Gene-expression analysis was performed by the ΔΔCt method (Müller et al., 2002), normalized for β-actin mRNA levels and expressed as mean ± S.D. ($n = 4$) relative to the value of control **RR** strain sample set as 1.

Protein Extraction and Western Blotting. Liver samples were placed into ice-cold PBS and then homogenized either in hypotonic buffer (10 mM Hepes pH 7.9, 1.5 mM MgCl$_2$, 5 mM KCl with 0.1% NP-40) for cytosolic proteins, in high-salt extraction buffer (20 mM Hepes pH 7.9, 25% glycerol, 450 mM KCl, 1 mM EDTA) for nuclear proteins or in RIPA buffer [50 mM Tris-HCl pH 7.5, 150 mM NaCl, 1% Triton X-100, 1% Na-deoxycholate, 0.1% sodium dodecyl sulfate (SDS)] for total proteins. Protease and phosphatase inhibitors [1 μg/ml aprotinin, 1 μg/ml leupeptin, 50 μg/ml phenylmethyl sulfonyl fluoride, 50 μg/ml Na$_3$VO$_4$, 1 mM dithiothreitol] were added to these buffers just before use. Proteins (50–100 μg) were separated in 7.5%–12% SDS-PAGE and transferred onto a nitrocellulose membrane (Protran; Schleicher & Schuell, Dassel, Germany). Membranes were first blocked in 5% milk in Tris-buffered saline and then incubated with anti-rabbit ALDH1/2 antibody (1:500; sc-50385; Santa Cruz; likely to detect at least ALDH1A1 and 1A7 isoforms that have similar molecular masses of 54 kDa), anti-mouse CAR (1:1000; PP-N4111-00; Perseus Proteomics; Tokyo, Japan), anti-mouse PXR (1:1000; PP-H4417-00; Perseus Proteomics). Goat anti-rabbit (sc-2004; Santa Cruz) and goat anti-mouse (sc-2005; Santa Cruz) horseradish peroxidase-conjugated antibodies were used as secondary antibodies at 1:5000 dilution. Immunodetection of bands was based on enhanced chemiluminescence kit (GE Healthcare, Little Chalfont, UK). Three independent sets of control, PB- or PCN-exposed rats were analyzed. Typical results from one set are shown in Figs. 1 and 2, and results of the remaining two sets are shown in the Supplemental Figs. 2 and 3.

ALDH1 Activity Assay. Liver samples were homogenized in ice-cold sucrose and centrifuged at 20, 000*g* for 30 minutes. Supernatants were used for the kinetic measurement of ALDH activity with propionaldehyde as substrate as described (Vasiliou and Marselos, 1989). This activity cannot distinguish between the cytosolic ALDH isoforms 1A1, 2, 3 and 7. Determination of the protein concentration was carried out according to the Lowry method (Lowry et al., 1951). The specific activities are expressed as mean ± S.D. of four animals per group.

Cloning of the ALDH1A7 Promoter and Reporter Constructs. Genomic DNA was isolated from liver tissue (25 mg) from 3-month-old male **RR** and **rr** rats according to the protocol of NucleoSpin tissue kit (Macherey-Nagel). The amplification of ~10 kilobase pair (kbp) fragments of *ALDH1A7* promoters (Rnor 5.0; Chr1:
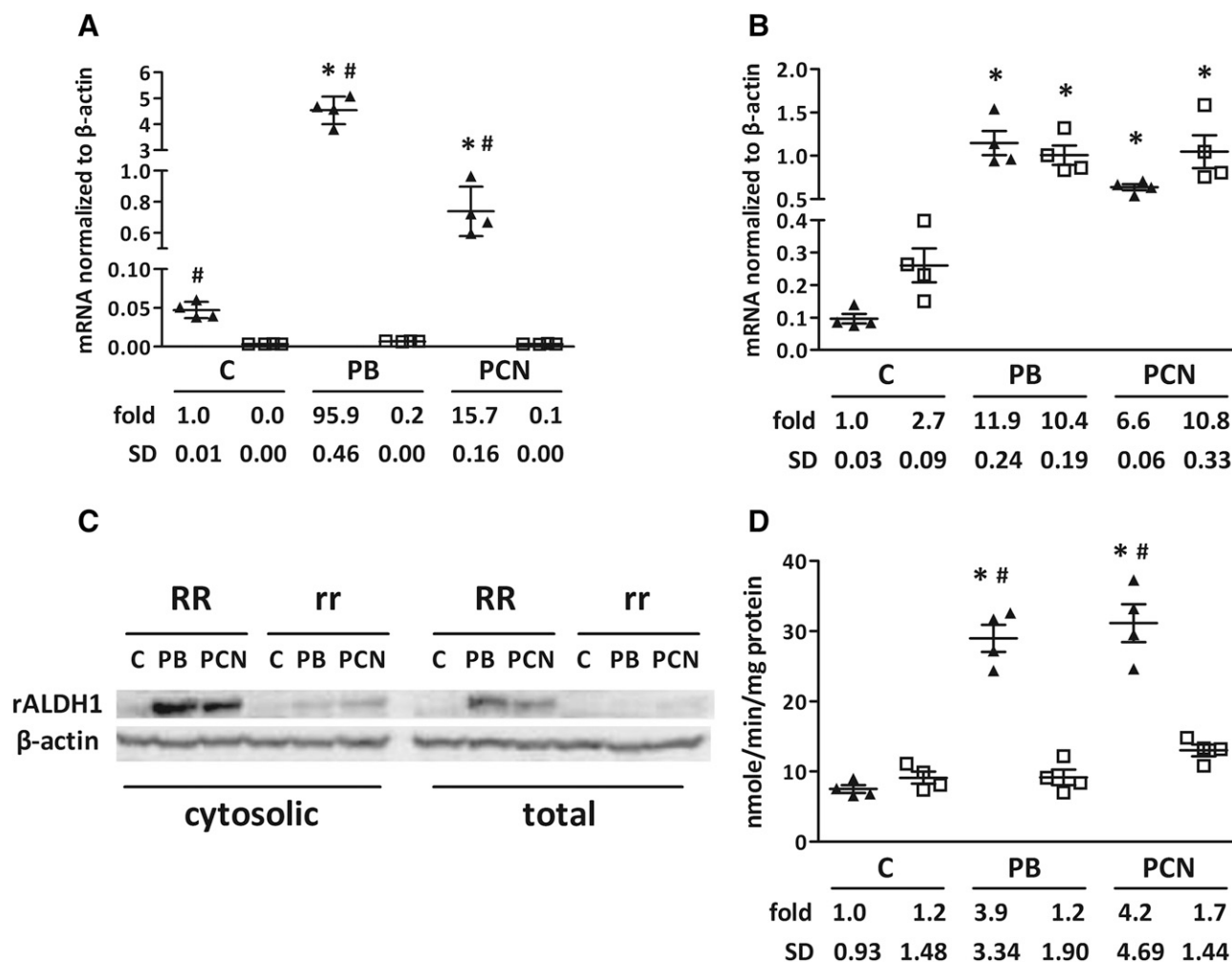
Fig. 1. Strain-dependent expression and inducibility of ALDH1A isoforms. Normalized expression of ALDH1A7 (A) and ALDH1A1 (B) mRNA in control, PB-, or PCN-treated **RR** and **rr** rat livers. Levels are expressed as scatter plots and means ± S.D. from four animals, each sample with two technical replicates. Cytosolic and total protein levels of ALDH1 protein (C) and activity (D) in control, PB-, or PCN-treated **RR** and **rr** rat livers. Statistically significant differences ($P < 0.05$) compared with the respective control group or between the strains are marked by * and # signs, respectively. The data in (A, B, and D) are also shown relative to the control RR values, set at 1.0, and expressed as means ± S.D. of -fold change below the x-axis.

247, 897, 931-247, 887, 931; reverse complement) from genomic DNA, and sequencing was done by Epoch Life Science Inc. (Missouri City, TX). The **RR** and **rr** promoter sequences have been submitted to the NCBI GenBank with accession numbers MK814117 and MK814118, respectively. The fragments were inserted into pGL3-Basic plasmid vectors (Promega, Madison, WI) at KpnI and XhoI restriction sites. Sequential deletion fragments of *ALDH1A7* promoters were generated by amplification with Phusion high-fidelity DNA polymerase (Finnzymes, Espoo, Finland) or KAPA HiFi (hot start) DNA polymerase (KAPA Biosystems) and forward and reverse primers (Oligomer, Helsinki, Finland) shown in Supplemental Table 1. The deletion fragments were cloned into pGL3-Basic plasmid vectors and competent *Escherichia coli* bacteria (XL-10 or DH5α) were transformed with the constructs. Colonies were screened by colony PCR using DreamTaq DNA polymerase (ThermoScientific, Vantaa, Finland). Plasmid DNAs from positive colonies were purified with QIAprep Spin Miniprep kit (Qiagen) and verified by dideoxy sequencing (DNA Analysis Facility, Yale University, New Haven, CT).

Reporter Gene Assays. The full-length mouse CAR and PXR constructs (Mäkinen et al., 2002) and the respective reporters (for CAR, PBREM-tk-luc; for PXR, XREM-3A4-luc) (Goodwin et al., 1999; Honkakoski et al., 2001) have been described earlier. C3A hepatoma cells were seeded on 48-well plates (~180,000 cells/cm²). The cells were transfected with the calcium phosphate method (Küblbeck

et al., 2008) with the appropriate combinations of the following three plasmids: one of the NR expression plasmids [full-length CAR, full-length PXR, or the empty expression vector (100 ng/well)], one of the reporter plasmids [individual *ALDH1A7* promoter construct, negative control pGL3-basic plasmid, positive control PBREM-tk-luc or XREM-3A4-luc reporters (450 ng/well)], *plus* the transfection control plasmid pCMVβ (900 ng/well). Untransfected cells served as blank samples for reporter enzyme assays. After transfection for 4 hours, the medium was removed and fresh DMEM supplemented with 5% delipidated serum (HyClone, Logan, UT) was added onto the transfected cells. The added medium also contained either the vehicle (DMSO, 0.1%) or activating NR ligands (1 μM TCPOBOP for mouse CAR; 10 μM RU486 for mouse PXR). After treatment with chemicals for 24 hours, the cells were lysed and assayed for luciferase and β-galactosidase activities as before (Honkakoski et al., 2001). Blank-subtracted luciferase activities were normalized, that is, divided, by blank-subtracted β-galactosidase activities and expressed relative to the empty pGL3-Basic reporter set at 1. Data are mean ± S.D. from three independent transfections.

Chromatin Immunoprecipitation Assay. Chromatin immunoprecipitation (ChIP) assays were performed according to Magklara and Smith (2009) with some modifications. Male 3-month-old **RR** and **rr** rats (two per condition) were injected with PB (80 mg/kg) or saline and killed by carbon dioxide asphyxiation 3 hours later. Liver
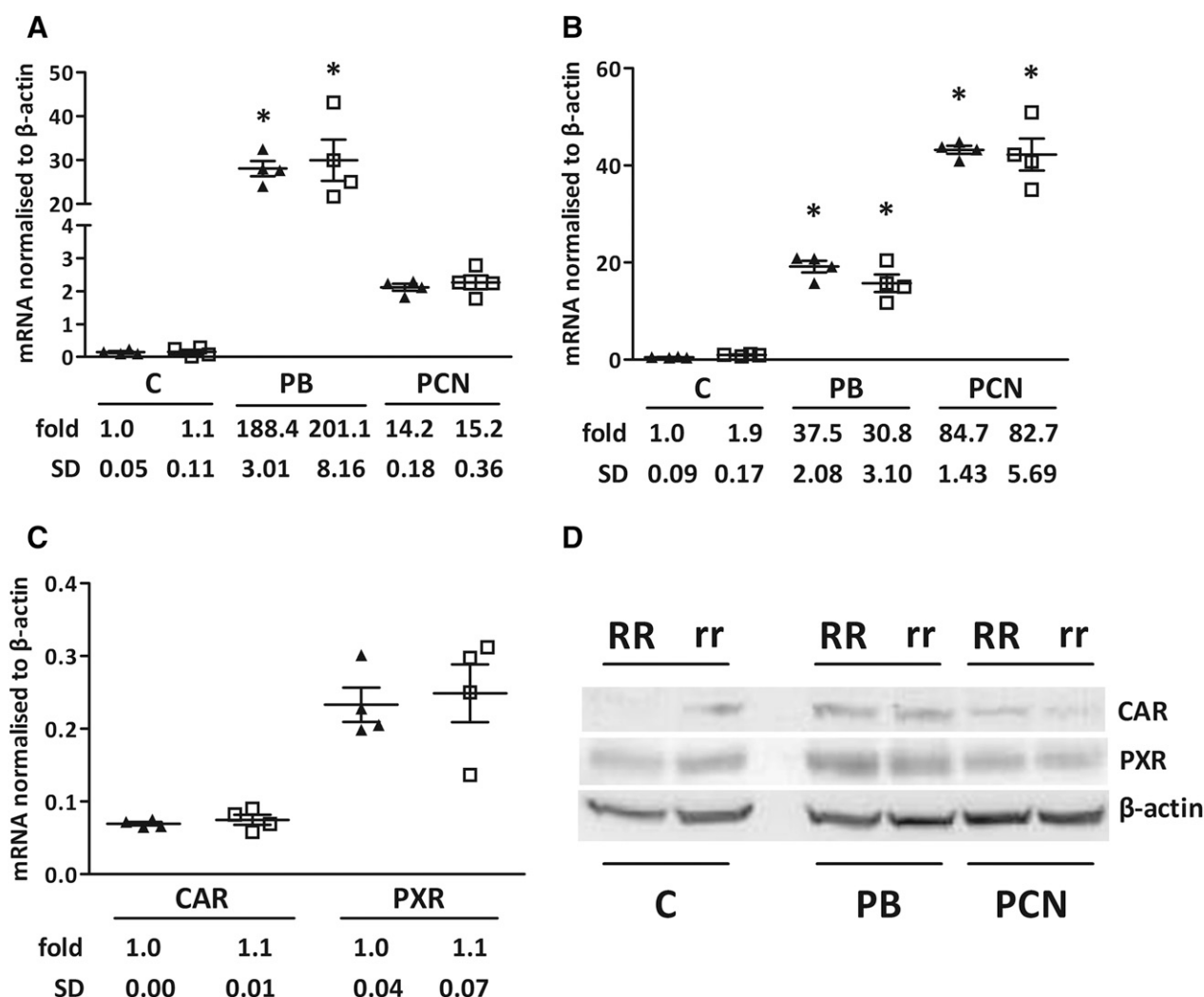
Fig. 2. Similar expression of CYP2Bs and NRs in both rat substrains. Normalized expression of CYP2B1 (A) and CYP3A23 (B) mRNA in control, PB-, or PCN-treated **RR** and **rr** rat livers. (C) Comparison of hepatic CAR and PXR mRNA expression between control rat strains. The ratio of target gene to β-actin mRNA expression (y-axis) are shown as scatter plots and means ± S.D. from four animals, each sample with two technical replicates. These normalized levels are also depicted as relative to the mean ± S.D. of the control **RR** strain, set at 1.0, and indicated below the x-axis. Statistically significant differences ($P < 0.05$) compared with the respective control group or between the strains are marked by * and # signs, respectively. (D) Expression of CAR and PXR proteins in control, PB- or PCN-treated **RR** and **rr** rat livers.

samples (80–100 mg) were fixed in 1% formaldehyde solution, and the cross-linking reaction was quenched by incubating the samples in 0.125 M glycine. The samples were then homogenized in sucrose buffer (0.3 M sucrose, 15 mM NaCl, 5 mM $MgCl_2$, 0.1 mM EDTA, 15 mM Tris-HCl, 0.5 mM dithiothreitol, 0.1 mM phenylmethyl sulfonyl fluoride) and centrifuged. The pelleted homogenates were resuspended in lysis buffer (50 mM Tris-HCl pH 8, 10 mM EDTA, 1% SDS) and incubated on ice for 10 minutes. Lysates were centrifuged and resuspended in sonication buffer (50 mM Hepes pH 7.5, 140 mM NaCl, 1 mM EDTA, 1% Triton-X, 0.1% Na-deoxycholate, 0.1% SDS). After sonication (80% power, 4 × 20 seconds with 1-minute cooling intervals; Misonix sonicator, Misonix, Inc., Farmingdale, NY), the DNA was sheared to an average length of 300–800 bp. The supernatants were diluted in ChIP dilution buffer (1.2 mM EDTA, 167 mM NaCl, 16.7 mM Tris-HCl pH 8, 1.1% Triton X-100, 0.01% SDS) and precleared with Protein A/G PLUS-agarose beads (sc-2003; Santa Cruz) at 4°C. Then, the beads were removed and 1/10 of the genomic DNA was retained as input control for quantitative PCR analysis. Precleared chromatin samples were incubated at 4°C overnight, with the addition of 5 μg polymerase II antibody (sc-899; Santa Cruz) or 5 μg of retinoid X receptor-α (RXRα) antibody (sc-553; Santa Cruz).

On the following day, protein-DNA complexes were precipitated after a 3-hour incubation with A/G beads. The beads were washed successively with low-salt buffer (2 mM EDTA, 20 mM Tris-HCl pH 8, 0.1% SDS, 1% Triton X-100, 150 mM NaCl), high-salt buffer (low-salt buffer with 500 mM NaCl), LiCl wash buffer (1 mM EDTA, 10 mM Tris-HCl pH 8, 1% Nonidet P-40, 1% Na-deoxycholate, 0.25 M LiCl) and twice with TE buffer (1 mM EDTA, 10 mM Tris-HCl pH 8). All buffers contained 1× protease inhibitor cocktail (P-27140; Sigma). After the two elution steps, the eluates and inputs were incubated with 5 M NaCl in 65°C overnight to reverse the DNA/protein crosslinks. After treatment with proteinase K (2 hours at 55°C), DNA was purified by phenol–chloroform-isoamyl alcohol extraction and ethanol precipitation. The DNA samples were analyzed by quantitative PCR in duplicate using KAPA SYBR FAST qPCR Master Mix (KK4601) and calculated by the $2^{-\Delta Ct}$ method after correcting for the IgG-negative control. The PCR primers used were synthesized by Eurofins Genomics (Ebersberg, Germany) and listed in the Supplemental Table 2.

Statistical Analysis. Differences between groups were evaluated by analysis of variance and Bonferroni's multiple comparison test. The main comparisons were between the strains and between the control

and inducer groups. Probability values $P < 0.05$ were considered statistically significant, but they are shown for descriptive purposes, not for hypothesis testing.

Results

Differential Expression of ALDH1A7 in RR and rr Rat Strains. Hepatic expression of *ALDH1A1* and *ALDH1A7* genes was studied after multiple doses of PB and PCN. Figure 1A shows that constitutive expression of rat ALDH1A7 mRNA was higher in the **RR** but still detectable in the **rr** rat strain. ALDH1A7 mRNA levels were induced more than 100-fold by PB and almost 20-fold by PCN only in the responsive **RR** strain, whereas no equivalent induction was detected in the **rr** strain. On the other hand, constitutive rat ALDH1A1 mRNA expression was only slightly higher in the **rr** strain whereas the induction of ALDH1A1 mRNA was comparable, reaching 4- to 10-fold by PB and 4- to 6-fold by PCN in both strains (Fig. 1B). Western blotting of cytosolic and total protein extracts (Fig. 1C; Supplemental Fig. 2) indicated low expression of ALDH1 proteins in control animals, whereas high expression levels were seen in PB-treated and moderate induction in PCN-treated **RR** rats only. It should be noted that the antibody used in Western blotting was the only one commercially available, and it does not distinguish between various ALDH1A isoforms. The ALDH1 (propionaldehyde/NAD$^+$) activity (Fig. 1D), catalyzed by all ALDH1A isozymes (Lindahl, 1992; Alnouti and Klaassen, 2008), displayed similar basal levels between the strains. It was elevated 3.5- and 4.5-fold by PB and PCN in the responsive **RR** rats, but it was only marginally elevated in the **rr** strain. These findings confirmed earlier reports on PB induction of both ALDH1A1 and 1A7 isoforms and the strain difference in ALDH1A7 inducibility by PB (Dunn et al., 1989; Pappas et al., 2001).

Expression of Inducible P450s and NRs in RR and rr Rats. Similar analyses revealed that hepatic transcripts of the main rat PB- and PCN-inducible *CYP2B1* and *CYP3A23* genes (Honkakoski and Negishi, 2000; Stanley et al., 2006) are detected in the untreated **RR** and **rr** animals at similar levels and are similarly induced by PB and PCN (Fig. 2, A and B). PB, an activator of rodent CAR, preferentially induced CYP2B1 over CYP3A23 mRNA. PCN, a ligand of rodent PXR, induced CYP3A23 over CYP2B1 mRNA expression, as expected. Furthermore, there was maximally only about a 2-fold change in the Ct values of β-actin mRNA between the control and induced groups (Supplemental Table 5), indicating that the observed strain differences and induction responses are not due to changes in the expression of the control gene used in normalization.

Furthermore, the expression of rat CAR and PXR mRNA (Fig. 2C) and the protein levels in total liver extracts (Fig. 2D; Supplemental Fig. 3) were also comparable. In time-course experiments, induction of ALDH1A1, ALDH1A7 (**RR** strain only), CYP2B1, and CYP3A23 mRNAs was clearly detectable 6 hours after PB or PCN injection, indicating a rapid transcriptional response (Supplemental Figs. 4 and 5). These results show that CAR and PXR receptors are present in both rat strains and function appropriately as regulators of *ALDH1A, CYP2B,* and *CYP3A* genes.

Comparison of ALDH1A7 Promoter Sequences in RR and rr Rats. The remarkable absence of ALDH1A7
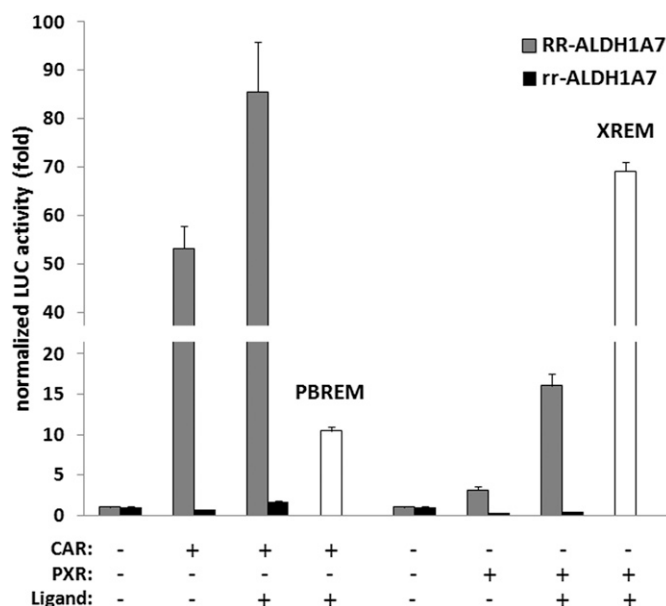

Fig. 3. Strain-dependent activation of *ALDH1A7* promoter constructs by NRs. Luciferase activity of the full-length **RR**-*ALDH1A7* (gray columns) and **rr**-*ALDH1A7* (black columns) constructs cotransfected with empty (−) or indicated CAR or PXR expression vectors (+), and treated with DMSO (ligand −) or selective CAR or PXR activators (ligand +). Positive control plasmids were PBREM-tk-luc for CAR and XREM-3A4-luc for PXR (white columns). Data are means ± S.D. from three independent transfections and expressed relative to the empty vector (set at 1.0). *Denotes a statistically significant difference from the empty vector at $P < 0.05$.

induction by PB, but normal expression and functionality of NRs in **rr** rats, suggested that the genetic difference in inducibility between the **RR** and **rr** strains may be related to changes in DNA sequences of their respective *ALDH1A7* genes. To study this hypothesis, genomic DNA from both strains was isolated, and ~10 kbp of *ALDH1A7* promoter fragments were amplified and sequenced. Alignment of the two promoter sequences showed that they are 97.6% identical (Supplemental Fig. 1), with the *ALDH1A7* sequence from the **rr** strain matching completely the available rat *ALDH1A7* sequence for *Rattus norvegicus* (ALDH1A7; Chr1:247, 847, 960-247, 887, 931 in the Rnor 5.0 assembly). Detailed comparison of the two *ALDH1A7* promoter sequences indicated that there were two larger deletions in the **rr** strain compared with the **RR** strain: one was a 165-bp region at ~2200 bp upstream of the transcription start site (TSS), missing in the **rr** strain. Another deletion (16 bp) occurred just upstream of the TATA box at −50/−34 bp. In addition, several small deletions and point mutations were present (Supplemental Fig. 1). With regard to transcription factor (TF) sites that could influence PB or PCN inducibility and/or hepatic expression of ALDH1A7 mRNA, we identified binding sites for CAR/RXRα sites, CCAAT box and DR3, DR4 and ER6 elements, which are shown in Supplemental Tables 3 and 4, respectively. None, however, showed a major difference between the **RR** and **rr** strains, and none was present in the above two deletion regions.

Activity of the Full-Length ALDH1A7 Promoters from RR and rr Rats. The 10-kbp *ALDH1A7* gene promoters were inserted into the pGL3-Basic reporter plasmid, co-transfected with mouse NR expression vectors into C3A hepatoma cells, and cells were treated with selective NR-activating ligands (Fig. 3). CAR and PXR activated the
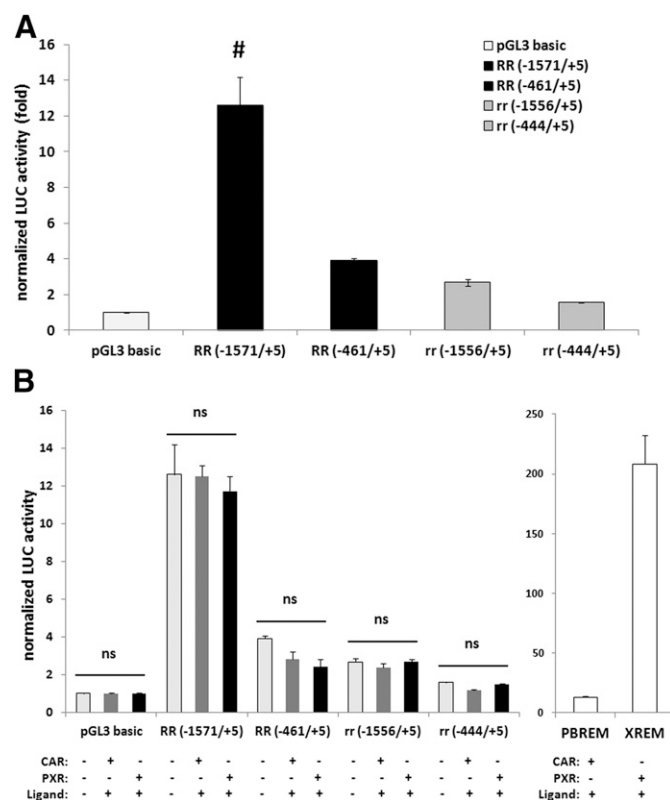
A

B

Fig. 4. Basal and NR-elicited activation of proximal *ALDH1A7* promoter constructs. (A) Basal luciferase reporter activity from **RR**-*ALDH1A7* and **rr**-*ALDH1A7* longer (−1571/+5 bp) and shorter (−461/+5 bp) promoter fragments. #Denotes a statistically significant different from the pGL3-Basic construct at $P < 0.05$; (B) NR-dependent luciferase activity from **RR**-*ALDH1A7* and **rr**-*ALDH1A7* longer and shorter promoter fragments in cotransfection assays with empty or indicated NR expression vectors. ns, no statistically significant differences between constructs with empty or NR expression vectors.

PBREM- and XREM-driven positive control reporters as expected (Mäkinen et al., 2002). The constitutively active CAR enhanced the activity of *ALDH1A7* promoter from the **RR** strain by ∼55-fold, and its ligand TCPOBOP further elevated the reporter activity over 80-fold compared with the pGL3-Basic control reporter, whereas the response to PCN-activated PXR was more modest, ∼16-fold increase; however, the *ALDH1A7* promoter from the **rr** strain was not appreciably affected by CAR or PXR. These findings correlate well with induction of ALDH1A7 mRNA (Fig. 1A) and indicate that the 10-kbp *ALDH1A7* **RR** promoter sequence harbors CAR- and PXR-responsive elements, whereas the **rr** promoter cannot be activated by these NRs.

Activity of the Proximal ALDH1A7 Promoters from RR and rr Rats. Because of the low ALDH1A7 expression in the **rr** strain, we turned our attention next to the proximal *ALDH1A7* promoter that contained several TF-binding sites, likely important for the constitutive activity, and the 16-bp deletion in the **rr** promoter. We measured the reporter activity and responsiveness to NRs of two proximal promoter fragments from both strains. Figure 4A shows that the longer (−1571/+5 bp)) **RR** fragment conferred a reporter activity of 12.5-fold over the promoterless control construct. Deletion to shorter **RR** fragment (−461/+5 bp) yielded an activity of about 30% of the longer fragment. The corresponding *ALDH1A7*
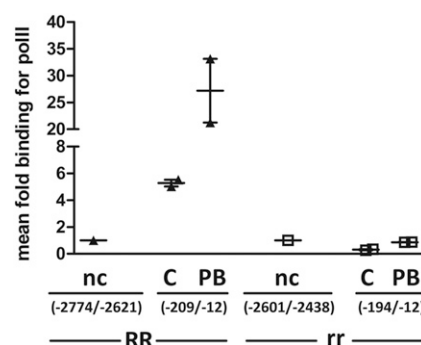

Fig. 5. Polymerase II binding to RR-*ALDH1A7* and rr-*ALDH1A7* proximal promoters. Both strains were dosed with saline (C) or PB for 3 hours; liver nuclear fractions were isolated and crosslinked, and RNA polymerase-associated DNA was analyzed by ChIP assay as detailed in *Materials and Methods*. The amount of recovered DNA is shown relative to the negative control (nc) region (set at 1.0). Data are scatter plots from two independent experiments, each sample with two technical replicates.

fragments from the **rr** strain had much weaker activities that tended to be on par or marginally above the pGL3-Basic construct. This finding indicates that the proximal *ALDH1A7* promoter (−444/+5 bp) in the **rr** strain contains defects that reduced the promoter activity and presumably decreased the expression of *ALDH1A7* gene.

Figure 4B shows results from the cotransfection assays with NR expression vectors and the proximal *ALDH1A7* fragments. In contrast to the 10-kbp **RR** promoter (Fig. 3), the more proximal fragments (**RR** −1571/+5 bp; **rr** −1556/+5 bp, or shorter) from either rat strain were not activated by ligand-activated CAR or PXR. This result indicates that the CAR/PXR-responsive element(s) lie in the far-upstream region of *ALDH1A7*.

Binding of Transcriptional Regulators to the ALDH1A7 Promoter Sequences. To shed more light on the differential expression of ALDH1A7 between **RR** and **rr** rats, we studied the binding of RNA polymerase II, an essential factor for RNA transcription, to the proximal *ALDH1A7* promoter and binding of NRs to the upstream regions. To this end, we used the ChIP assay with chromatin samples extracted from both strains exposed to vehicle or PB.

We detected significant RNA polymerase II binding (>6-fold over background) to the proximal promoter region (−209/−12 bp) in samples from control **RR** rats. This binding was clearly elevated by PB (Fig. 5). In contrast, RNA polymerase II showed weak or no binding to the corresponding fragment (−194/−12 bp) from **rr** rats, regardless of treatment. This finding provides strong support to our hypothesis that the *ALDH1A7* gene has an active and PB-responsive promoter in **RR** rats, whereas its activity is low and noninducible in the **rr** strain.

Next, we sought to identify the locations of the CAR binding sites in the *ALDH1A7* far-upstream region. Because the available CAR antibody was not suitable for ChIP assays, we used instead an antibody to RXRα, the obligate hetero-dimer partner of CAR and PXR for DNA binding (Honkakoski and Negishi, 2000). A similar approach of using RXRα as a surrogate for CAR binding was taken in previous studies (Saito et al., 2013; Ohno et al., 2014). Inspection of NR binding sites with direct or everted repeats of AGGTCA-like motifs with the NUBIScan algorithm (Podvinec et al., 2002) revealed three putative CAR/RXRα binding sites at −3075 (named
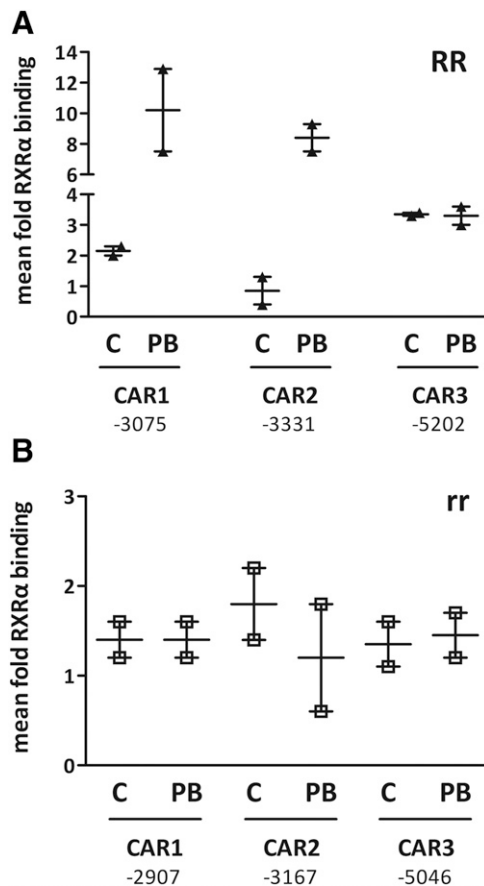
Fig. 6. RXRα binding to putative CAR binding sites in the distal regions of RR-*ALDH1A7* (A) and rr-*ALDH1A7* (B) promoters. Both strains were dosed with saline (C) or PB for 3 hours, and liver nuclear fractions were isolated and crosslinked, and RXRα- associated DNA was analyzed by ChIP assay as detailed in *Materials and Methods*. The amount of recovered DNA is shown relative to the negative control region (set at 1.0). Data are scatter plots from two independent experiments, each sample with two technical replicates.

CAR1), at −3331 (named CAR2) and at −5202 (named CAR3) for the *RR* strain (the respective locations are −2907, −3167, and −5046 for the *rr* strain). Sequence comparison of these sites between the *RR* and *rr* strains showed no major differences, apart from a single point mutation in the CAR-RXRα binding CAR1 site (a DR4 element). There were also three other putative CAR/RXRα binding sites (upstream from −8300 in *RR*); however, they have shown no significant ChIP binding (data not shown).

In Fig. 6A, binding of RXRα was detectable to all three CAR/RXRα binding sites in chromatin samples isolated from control *RR* rats. Exposure to PB substantially enhanced RXRα binding to CAR1 and CAR2 sites (5- and 10-fold, respectively), whereas the increase was lower at the CAR3 site (2-fold). Experiments performed with chromatin from the *rr* rats (Fig. 6B) showed low binding both in control and PB-treated samples.

Discussion

The present study provides evidence for the molecular basis underlying the differences in PB inducibility of ALDH activity observed in *RR* and *rr* rat strains. We showed that the low ALDH activity in the nonresponsive *rr* strain is associated with the lack of ALDH protein and mRNA expression. This difference cannot be attributed to defects in the PB induction process itself because expression of the CAR regulator and inducibility of the ALDH1A1, CYP2B1, and CYP3A23 mRNAs were comparable in the two strains. We also showed, for the first time, that the rat *ALDH1A7* gene is regulated by PXR and its ligand, albeit to a lesser extent than by CAR.

Reporter gene assays using *ALDH1A7* promoter fragments indicated that whereas the largest (10-kbp) fragment from the *RR* rats was strongly activated by CAR and PXR, the corresponding *rr* fragment was practically inactive. Other experiments indicated that the proximal *rr* promoter is clearly weak and cannot recruit RNA polymerase as efficiently as the *RR* promoter. Apart from a few dispersed point mutations and deletions at positions that did not seem to affect any predicted TF binding site, there is a 16-bp *RR* sequence at −50/−34 bp, very close to the predicted TATA box, that is lacking in *rr* rats. This 16-bp sequence is quite similar to a recognition element of the general transcription factor TFIIB (Littlefield et al., 1999), and this site is essential for recruitment of the RNA polymerase II. Accordingly, RNA polymerase II failed to bind to the fragment −194/−12 bp in chromatin samples from the *rr* rats. Based on the present findings, we suggest that the 16-bp deletion is the ultimate reason for the low ALDH1A7 activity and inducibility by PB in the nonresponsive *rr* rats.

Upstream regions at −3050 and −3300 bp harbored sites capable of NR binding as indicated by efficient recruitment of RXRα, which is essential for the CAR-dependent transcription. Whereas robust RXRα binding to the *RR* gene took place especially after PB administration, binding to the *rr* gene was detected only at low levels and not affected by PB. This is quite surprising given the fact that the NR binding sites in the *rr* gene were intact. This finding suggests that CAR binding to these distal sites may require priming, that is, appropriate recruitment of factors binding to the proximal *ALDH1A7* promoter before CAR binding can occur. This implies that the inability of the proximal *ALDH1A7 rr* promoter to recruit general TFs may also result in reversion of distal CAR binding sites into a transcriptionally inactive state in the *rr* rats. There is similar evidence that mutations in a single regulatory sequence can affect the accessibility to TFs of the entire gene locus (Kumasaka et al., 2016).

The genome-wide chromatin accessibility and inducibility by TCPOBOP have recently been investigated in mice. The *Cyp2b10* and *Aldh1a7* genes belong to a group termed *pattern 1,* where TCPOBOP produces stronger induction than PCN (Cui and Klaassen, 2016). In the *Cyp2b10* gene upstream sequence, there is low but detectable CAR/RXR binding in control animals that is enhanced by 6- to 8-fold after TCPOBOP exposure (Tian et al., 2018). These data correlate well with our findings on the *RR ALDH1A7* gene. The murine *Aldh1a7* locus contains an active promoter, as evidenced by activating histone H3K4me3 and H3K27Ac marks (Sugathan and Waxman, 2013) and a TCPOBOP-responsive DNase I hypersensitive site (Lodato et al., 2018) overlapping the TSS, a finding that matches well with the active rat *ALDH1A7* proximal promoter in *RR* rats. The far-upstream DNase I hypersensitive sites are located at

~17 and ~29 kbp upstream of the *Aldh1a7* TSS but still within the same topologically associated domain (Lodato et al., 2018).

In contrast, information on genome chromatin accessibility or epigenetics in the rat liver is quite sparse. The available data [https://www.ebi.ac.uk/arrayexpress: accession number E-MTAB-2663] show that the rat *ALDH1A1* gene possesses strong activating histone marks (H3K4me3 and H3K27Ac) that overlap the *ALDH1A1* TSS and the first exon (Villar et al., 2015). The co-occurrence of these two histone modifications is indicative of an active promoter, in line with a robust ALDH1A1 mRNA expression in both *rr* and *RR* strains; however, in the same data set, coinciding H3K4me3 and H3K27Ac marks closest to the *ALDH1A7* gene are more than 200 kbp away from its TSS, which correlates with the low expression of ALDH1A7 mRNA. It should be noted again that the rat reference genome (Rnor 5.0) used in these studies contains the *rr* strain *ALDH1A7* sequence.

Collectively, our results show that PB induces ALDH1A7 expression at activity, protein, and mRNA level in only the responsive *RR* rats via binding of CAR to upstream elements in *ALDH1A7*, which is inherently associated with enhanced recruitment of RNA polymerase II to the proximal promoter. Because of sequence variation between these rat strains, the expression and accumulation of ALDH1A7 mRNA are disrupted in the nonresponsive *rr* rats, which likely also affects ALDH1A7-inducing signals other than PB that act via transcriptional activation.

The human relevance of our findings is still unclear. *ALDH1A7* is not present in the human genome as it is thought to be a rodent-specific duplication of the ancestral *ALDH1A1* gene. There are no direct publications on PB inducibility of human *ALDH1A1*, whereas rodent *ALDH1A1* and *1A7* genes are both activated. We found an RNA sequencing data set of human HepaRG cells exposed to human CAR- and PXR-activating CITCO and PB (Li et al., 2015; GeoExpress GSE71446) that showed a substantial 3.5- to 16-fold increase in CYP2B6 and CYP3A4 mRNAs but only a slight increase (<40%) in ALDH1A1 mRNA expression.

In conclusion, we consider that the present data have shed light on the 40-year conundrum of strain differences in ALDH inducibility by PB. They also suggest that metabolism of endogenous and exogenous aldehydes may be attenuated in rat strains harboring this genetic defect, which could have consequences for the design and interpretation of biologic, pharmacological and toxicological studies on functions and disposition of aldehydes.

Authorship Contributions

Participated in research design: Touloupi, Küblbeck, Magklara, Molnár, Reinisalo, Honkakoski, Pappas.

Conducted experiments: Touloupi, Küblbeck, Molnár, Reinisalo, Konstandi, Pappas.

Performed data analysis: Touloupi, Küblbeck, Magklara, Reinisalo, Honkakoski, Pappas.

Wrote or contributed to the writing of the manuscript: Touloupi, Magklara, Honkakoski, Pappas.

References

Aleksunes LM and Klaassen CD (2012) Coordinated regulation of hepatic phase I and II drug-metabolizing genes and transporters using AhR-, CAR-, PXR-, PPARα-, and Nrf2-null mice. *Drug Metab Dispos* 40:1366–1379.

Alnouti Y and Klaassen CD (2008) Tissue distribution, ontogeny, and regulation of aldehyde dehydrogenase (Aldh) enzymes mRNA by prototypical microsomal enzyme inducers in mice. *Toxicol Sci* 101:51–64.

Chai X, Zeng S, and Xie W (2013) Nuclear receptors PXR and CAR: implications for drug metabolism regulation, pharmacogenomics and beyond. *Expert Opin Drug Metab Toxicol* 9:253–266.

Cui JY and Klaassen CD (2016) RNA-Seq reveals common and unique PXR- and CAR-target gene signatures in the mouse liver transcriptome. *Biochim Biophys Acta* 1859:1198–1217.

Deitrich RA (1971) Genetic aspects of increase in rat liver aldehyde dehydrogenase induced by phenobarbital. *Science* 173:334–336.

Dunn TJ, Koleske AJ, Lindahl R, and Pitot HC (1989) Phenobarbital-inducible aldehyde dehydrogenase in the rat. cDNA sequence and regulation of the mRNA by phenobarbital in responsive rats. *J Biol Chem* 264:13057–13065.

Goodwin B, Hodgson E, and Liddle C (1999) The orphan human pregnane X receptor mediates the transcriptional activation of CYP3A4 by rifampicin through a distal enhancer module. *Mol Pharmacol* 56:1329–1339.

Honkakoski P, Jääskeläinen I, Kortelahti M, and Urtti A (2001) A novel drug-regulated gene expression system based on the nuclear receptor constitutive androstane receptor (CAR). *Pharm Res* 18:146–150.

Honkakoski P, Moore R, Gynther J, and Negishi M (1996) Characterization of phenobarbital-inducible mouse *Cyp2b10* gene transcription in primary hepatocytes. *J Biol Chem* 271:9746–9753.

Honkakoski P and Negishi M (2000) Regulation of cytochrome P450 (*CYP*) genes by nuclear receptors. *Biochem J* 347:321–337.

Hsu LC, Chang WC, Hoffmann I, and Duester G (1999) Molecular analysis of two closely related mouse aldehyde dehydrogenase genes: identification of a role for *Aldh1*, but not *Aldh-pb*, in the biosynthesis of retinoic acid. *Biochem J* 339: 387–395.

Jackson B, Brocker C, Thompson DC, Black W, Vasiliou K, Nebert DW, and Vasiliou V (2011) Update on the aldehyde dehydrogenase gene (*ALDH*) superfamily. *Hum Genomics* 5:283–303.

Kathmann EC, Naylor S, and Lipsky JJ (2000) Rat liver constitutive and phenobarbital-inducible cytosolic aldehyde dehydrogenases are highly homologous proteins that function as distinct isozymes. *Biochemistry* 39:11170–11176.

Küblbeck J, Jyrkkärinne J, Poso A, Turpeinen M, Sippl W, Honkakoski P, and Windshügel B (2008) Discovery of substituted sulfonamides and thiazolidin-4-one derivatives as agonists of human constitutive androstane receptor. *Biochem Pharmacol* 76:1288–1297.

Kumasaka N, Knights AJ, and Gaffney DJ (2016) Fine-mapping cellular QTLs with RASQUAL and ATAC-seq. *Nat Genet* 48:206–213.

Li D, Mackowiak B, Brayman TG, Mitchell M, Zhang L, Huang SM, and Wang H (2015) Genome-wide analysis of human constitutive androstane receptor (CAR) transcriptome in wild-type and CAR-knockout HepaRG cells. *Biochem Pharmacol* 98:190–202.

Lindahl R (1992) Aldehyde dehydrogenases and their role in carcinogenesis. *Crit Rev Biochem Mol Biol* 27:283–335.

Littlefield O, Korkhin Y, and Sigler PB (1999) The structural basis for the oriented assembly of a TBP/TFB/promoter complex. *Proc Natl Acad Sci USA* 96:13668–13673.

Lodato NJ, Rampersaud A, and Waxman DJ (2018) Impact of CAR agonist ligand TCPOBOP on mouse liver chromatin accessibility. *Toxicol Sci* 164:115–128.

Lowry OH, Rosebrough NJ, Farr AL, and Randall RJ (1951) Protein measurement with the Folin phenol reagent. *J Biol Chem* 193:265–275.

Magklara A and Smith CL (2009) A composite intronic element directs dynamic binding of the progesterone receptor and GATA-2. *Mol Endocrinol* 23:61–73.

Mäkinen J, Frank C, Jyrkkärinne J, Gynther J, Carlberg C, and Honkakoski P (2002) Modulation of mouse and human phenobarbital-responsive enhancer module by nuclear receptors. *Mol Pharmacol* 62:366–378.

Marselos M (1976) Genetic variation of drug-metabolizing enzymes in the wistar rat. *Acta Pharmacol Toxicol (Copenh)* 39:186–197.

Marselos M, Strom SC, and Michalopoulos G (1987) Effect of phenobarbital and 3-methylcholanthrene on aldehyde dehydrogenase activity in cultures of HepG2 cells and normal human hepatocytes. *Chem Biol Interact* 62:75–88.

Müller PY, Janovjak H, Miserez AR, and Dobbie Z (2002) Processing of gene expression data generated by quantitative real-time RT-PCR. *Biotechniques* 32: 1372–1374, 1376, 1378–1379.

Ohno M, Kanayama T, Moore R, Ray M, and Negishi M (2014) The roles of co-chaperone CCRP/DNAJC7 in *Cyp2b10* gene activation and steatosis development in mouse livers. *PLoS One* 9:e115663.

Pappas P, Stephanou P, Karamanakos P, Vasiliou V, and Marselos M (2001) Phenobarbital inducibility and differences in protein expression of an animal model. *Chem Biol Interact* 130–132:275–283.

Pappas P, Stephanou P, Vasiliou V, and Marselos M (1998) Zoxazolamine-induced paralysis in two rat substrains: differences in hepatic drug metabolism. *Eur J Drug Metab Pharmacokinet* 23:461–467.

Podvinec M, Kaufmann MR, Handschin C, and Meyer UA (2002) NUBIScan, an *in silico* approach for prediction of nuclear receptor response elements. *Mol Endocrinol* 16:1269–1279.

Saito K, Moore R, and Negishi M (2013) Nuclear receptor CAR specifically activates the two-pore K$^+$ channel Kcnk1 gene in male mouse livers, which attenuates phenobarbital-induced hepatic hyperplasia. *Toxicol Sci* 132:151–161.

Sophos NA, Pappa A, Ziegler TL, and Vasiliou V (2001) Aldehyde dehydrogenase gene superfamily: the 2000 update. *Chem Biol Interact* 130–132:323–337.

Stanley LA, Horsburgh BC, Ross J, Scheer N, and Wolf CR (2006) PXR and CAR: nuclear receptors which play a pivotal role in drug disposition and chemical toxicity. *Drug Metab Rev* 38:515–597.

Sugathan A and Waxman DJ (2013) Genome-wide analysis of chromatin states reveals distinct mechanisms of sex-dependent gene regulation in male and female mouse liver. *Mol Cell Biol* **33**:3594–3610.

Tian J, Marino R, Johnson C, and Locker J (2018) Binding of drug-activated CAR/Nr1i3 alters metabolic regulation in the liver. *iScience* **9**:209–228.

Vasiliou V and Marselos M (1989) Tissue distribution of inducible aldehyde dehydrogenase activity in the rat after treatment with phenobarbital or methylcholanthrene. *Pharmacol Toxicol* **64**:39–42.

Villar D, Berthelot C, Aldridge S, Rayner TF, Lukk M, Pignatelli M, Park TJ, Deaville R, Erichsen JT, Jasinska AJ, et al. (2015) Enhancer evolution across 20 mammalian species. *Cell* **160**:554–566.

Westerlund M, Galter D, Carmine A, and Olson L (2005) Tissue- and species-specific expression patterns of class I, III, and IV Adh and Aldh 1 mRNAs in rodent embryos. *Cell Tissue Res* **322**:227–236.

Address correspondence to: [1]Paavo Honkakoski, School of Pharmacy, Pharmaceutics, University of Eastern Finland, Yliopistonranta 1 C, P.O. Box 1627Kuopio, FI-70211, Finland. E-mail: phonka@email.unc.edu or [2]Periklis Pappas, Faculty of Medicine, School of Health Sciences, University of Ioannina, 45110 Ioannina, Greece. E-mail: ppappas@cc.uoi.gr